Chemical Engineering Journal 152 (2009) 88–94

Contents lists available at ScienceDirect

Chemical Engineering Journal

journal homepage: www.elsevier.com/locate/cej

Coagulation removal of melanoidins from biologically treated molasses wastewater using ferric chloride

Zhen Liang [a,b], Yanxin Wang [b,*], Yu Zhou [b], Hui Liu [b]

[a] State Key Laboratory of Freshwater Ecology and Biotechnology, Institute of Hydrobiology, Chinese Academy of Sciences, Wuhan 430072, China
[b] MOE Key Laboratory of Biogeology and Environmental Geology and School of Environmental Studies, China University of Geosciences, 430074 Wuhan, China

ARTICLE INFO

Article history:
Received 19 August 2007
Received in revised form 14 March 2009
Accepted 22 March 2009

Keywords:
Molasses wastewater
Ferric chloride
Coagulation performance
Molecular weight
Floc size distribution
Mechanism

ABSTRACT

The pigments (melanoidins) in molasses wastewater are refractory to conventional biological treatment. Ferric chloride was used as coagulant to remove color and chemical oxygen demand (COD) from molasses effluent. Using jar test procedure, main operating conditions such as pH and coagulant dosage were investigated. Under the optimum conditions, up to 86% and 96% of COD and color removal efficiencies were achieved. Residual turbidity in supernatant was less than 5 NTU and Fe^{3+} concentration was negligible because of effective destabilization and subsequent sedimentation. The results of high performance size exclusion chromatography (HPSEC) show that low molecular weight (MW) fraction of melanoidins is more reactive than high MW fraction and increase in the concentration of the lowest MW organic group is related to the capacity of charge neutralization. Aggregate size measurement reveals the size effect on the settleability of flocs formed, with larger flocs settling more rapidly. Charge neutralization and co-precipitation are proposed as predominant coagulation mechanism under the optimum conditions.

1. Introduction

Molasses, a by-product of sugar production, is the most common raw material for fermentation industries such as baker's yeast and ethanol production because of its low cost and high content of sugar. However, one major problem faced in this fermentation process is the generation of large quantity of wastewater with high organic pollutant loading and dark brown color.

Conventional biological processes, typically anaerobic digestion and activated sludge, are effective in removing biochemical oxygen demand (BOD) from molasses wastewater. However, the brown color remains or even darkens in the biologically treated effluent due to repolymerization of pigments [1]. The colored compounds, known as melanoidins, are formed during the non-enzymatic browning reaction (Millard reaction) between amino compounds and carbohydrates. As a type of high molecular weight polymers in nature [2], melanoidins are anti-oxidant and thus recalcitrant to bio-degradation. Melanoidins in the treated effluent are hazardous in that they prevent sunlight penetration and reduce both photosynthetic activity and dissolved oxygen level of surface waters [3].

Different approaches such as membrane processes [4], chemical oxidation using ozone [5], Fenton reagent [6] and supercritical water oxidation [7] have been tested to remove COD and color from molasses effluent. Besides, certain microorganisms, such as white rot fungi, have been found capable of degrading melanoidins under nutrient limitation conditions [8]. These methods, however, are commonly associated with less effective decolorization rate, high equipment and operational cost, and simultaneous generation of by-products which are potentially more hazardous [9]. Up to date, none of the methods have been successfully applied in the treatment of molasses wastewater. Therefore, cost-effective techniques are urgently needed for the advanced treatment of molasses wastewater.

Coagulation–flocculation is an essential unit process in removing colloidal particles and natural organic matters (NOM) in water [10] and wastewater treatment [11]. Since melanoidins are chemically similar to NOM, this process is possibly applicable to remove melanoidins. Aluminum-based salts and iron-based salts are the most commonly used coagulants. Iron salts have been reported to be more effective than alum salts in the removal of dissolved organic carbons. In addition, public health concern has recently arisen about residual alum ion levels in the coagulated water which have additional risk of development of Alzheimer's disease. In recent years, we have experimentally tested the viability of cellular iron for decolorization of dyeing wastewater [12]. Therefore, ferric chloride, a conventional coagulant, was selected in this work for

* Corresponding author. Tel.: +86 27 67883998; fax: +86 27 87481030.
E-mail address: yx.wang@cug.edu.cn (Y. Wang).

1385-8947/$ – see front matter © 2009 Elsevier B.V. All rights reserved.
doi:10.1016/j.cej.2009.03.036

the polishing treatment of biologically treated molasses wastewater.

Migo et al. [13] reported decolorization of molasses wastewater using polyferric sulfate. Ryan et al. [14] compared electrocoagulation with coagulation in the effectiveness of removing residual color and COD from molasses process water. However, optimization of the most influential parameters, such as pH and coagulant dosage, has yet to be established. As a part of an extensive research project aiming at establishing national standards of wastewater discharge in yeast industry in China, the objectives of this study are to test the feasibility of removing COD and color from biologically treated molasses wastewater using ferric chloride and to investigate main operating parameters such as pH and coagulant dose that influence coagulation performance. Molecular weight of organic compounds was determined using HPSEC and floc size was measured using light scattering technique. Coagulation mechanism under the optimal conditions is proposed. The experimental results are important for providing basic parameters serving the coagulation technique of bio-treated molasses wastewater.

2. Experimental

2.1. Materials and methods

Molasses wastewater was taken from a yeast manufacturing factory located in Hubei province of China. The factory has a full-scale two-staged biological treatment facility. Samples under investigation were collected from a single batch of aerobically treated effluents. All samples were stored in 25 L plastic carboys and kept in refrigerator at 5 °C before use.

Ferric chloride was of analytical grade and prepared as 250 g/L stock solution by dissolving ferric chloride into distilled water.

2.2. Coagulation procedure

Coagulation/flocculation tests were conducted using a conventional jar test apparatus (TA-6, China). For each trial, 500 mL samples were poured into 1 L beakers. The pH was adjusted to desired value using concentrated sulfuric acid or sodium hydroxide. Coagulant was added and jar tests began with rapid mixing at 500 rpm for 1 min, followed by slow agitation of 60 rpm for 10 min. The flocs formed were then allowed to settle. The end of sedimentation was set at a time when no appreciable settlement of flocs was observed. Finally, approximately 150 mL samples were withdrawn with a plastic syringe from near 2 cm below liquid–air interface for chemical analysis. All the experiments were carried out at ambient temperature (25–28 °C).

2.3. HPSEC

The molecular weight distribution of molasses pigments was determined using HPSEC. The samples were first filtered through a 0.45 μm membrane and then HPSEC fractionated with a Hewlett-Packard HPLC 1100-series system, equipped with a refractive index (RI) detector (G1362A, Agilent) and a PL aquagel-OH column (product number: 79911GF-083, Agilent). Deionized water was used as eluent at a flow rate of 1 mL/min. Injection volume was 5 μL. The data were processed with ChemStation software.

2.4. Floc size measurement

Immediately after rapid mixing step, 5 mL flocs was collected from sampling hole of the beaker and diluted to 50 mL with distilled water to prevent further agglomeration. Floc size distribution was measured using a laser grain-size analyzer (LS230, USA).

Table 1
Properties of the biologically treated molasses effluent.

Parameter	Units	Range
pH		7.9–8.1
COD	mg/L	950–1000
BOD_5	mg/L	20–25
Color	Abs/cm	1.3–1.4
Turbidity	NTU	20–25
Alkalinity[a]	mg/L	1800–1950
Cl^-	mg/L	1500–1700
SO_4^{2-}	mg/L	240–260

[a] Alkalinity expressed as CaO.

2.5. Analytic method

The pH value was measured with a bench-scale pH meter (PHS-25, China). Calibration was regularly carried out with pH 6.86 and pH 4.00 standard buffers. COD was measured by closed-reflux method using dichromate as oxidant. BOD was measured in accordance with national standards [15]. Dissolved oxygen (DO) was determined using a portable DO meter (YSI 55, USA). Color was expressed as optical density and measured at the absorbance of 475 nm, a wavelength that characterizes brown color, using a spectrophotometer (722S, China). The pH of sample was adjusted to 5 with concentrated sulfuric acid or sodium hydroxide solution and centrifuged at 4000 rpm for 20 min prior to spectrophotometric measurement. Turbidity was directly read on a turbidity meter (TDT-2, China) in nephelometric turbidity unit, NTU. Zeta potential was assayed using a zeta meter (Nano-2S90 Zeta Sizer). A phenanthroline method was used to analyze both ferrous iron and total iron concentration in coagulated effluent [16].

3. Results and discussion

3.1. Wastewater characterization

Aerobically treated molasses effluent is weakly alkaline, low in BOD but high in COD. The main characteristics of this effluent are listed in Table 1.

The change in zeta potential with pH is presented in Fig. 1. Zeta potential decreases with increase in effluent pH. This pH-dependent phenomenon is probably due to the deprotonation of acidic organic functional groups, such as carboxylic acid, present in melanoidins:

$$COOH \rightarrow COO^- + H^+ \quad (1)$$

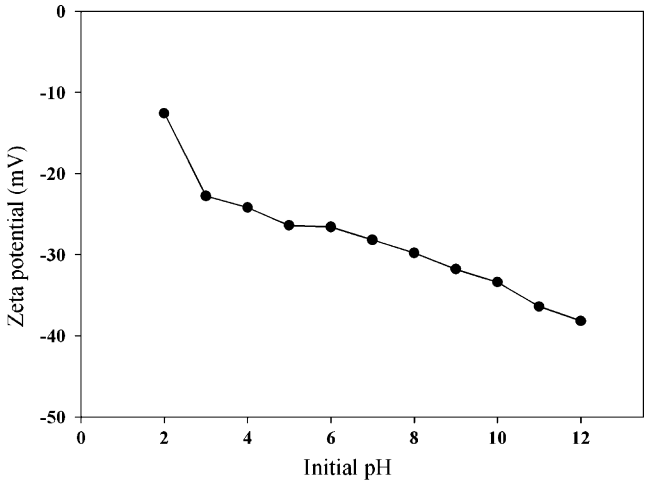

Fig. 1. Zeta potential as a function of effluent pH.

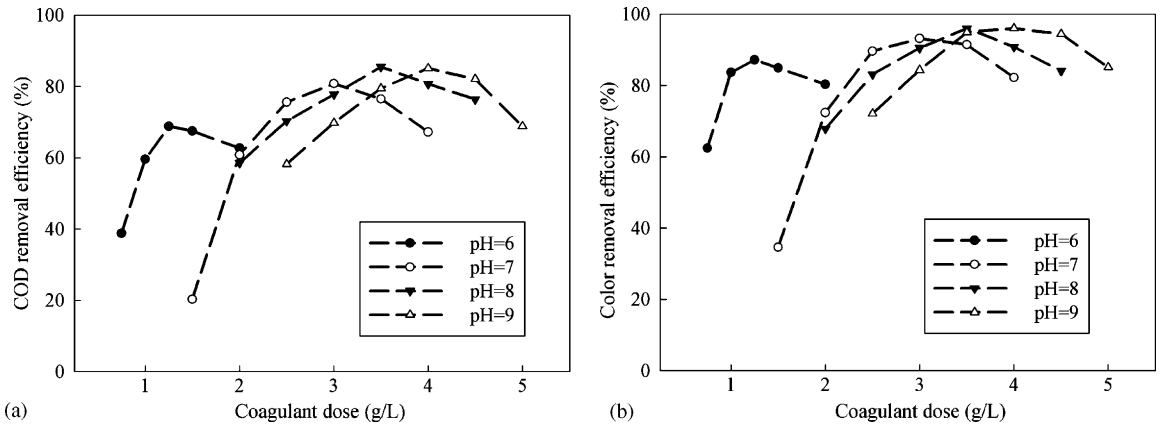

Fig. 2. Removal efficiencies as functions of coagulant dose and pH: (a) COD removal and (b) color removal.

Increase in pH facilitates deprotonation process, thus resulting in more negatively charged effluent. Zeta potential retained negative in the whole pH range tested and the raw effluent was highly negatively charged (−30 mV). Since large amount of coagulant is required for co-precipitation of carboxylic groups [17], substantial iron demand is expected.

3.2. Effect of coagulant dose and pH on COD and color removals

Visual inspection of coagulated effluent indicates that iron dosage varies greatly with initial pH. Therefore, different dosage range was tested with varying initial pH levels.

COD removal efficiency as a function of coagulant dose at different initial pH is given in Fig. 2(a). The curves of COD removal show a common tendency: removal efficiency first rises with increasing coagulant dose, reaching the maximal value, and then decreases with further coagulant addition. The optimum coagulant dose (OCD) in this study is defined as the lowest coagulant dosage at which maximum COD removal efficiency is achieved. As shown in Fig. 2(a), the OCDs in the pH range of 7–9 were 3.0 g/L, 3.5 g/L and 4.0 g/L, respectively, but the OCD was only 1.25 g/L at pH 6. On the other hand, less satisfactory COD removal efficiency (69%) is attained at pH 6 compared to those at higher pH levels (>80%).

The tendency of decolorization curves is consistent with that of COD removal and the optimum doses for decolorization rates coincide with the OCDs in the pH range tested (Fig. 2(b)). Almost complete color removal (96%) was achieved at OCD for raw effluent, implying that melanoidins can be successfully reduced by coagulation. Besides, organic removal accompanied by decolorization confirms that melanoidins constitute major portion of organic compounds in bio-treated molasses wastewater. Similar to COD removal, decolorization rate in the pH range of 7–9 is significantly higher than at pH 6. Visual inspection also reveals much light-colored supernatant at higher pH compared to that at pH 6 at the OCDs. Therefore, initial pH of molasses effluent should at least be neutral to maintain a more stable COD (color) removal efficiency.

3.3. Effect of coagulant dose and pH on residual turbidity and ferric concentration

Iron dosage corresponding to the lowest residual turbidity coincides with the OCD for all the pH values tested, as shown in Fig. 3(a). Moreover, the better the removal efficiency, the lower the residual turbidity. For instance, the lowest turbidity was less than 10 NTU in the pH range of 7–9, compared to 53 NTU at pH 6, a value even higher than that without coagulation.

Iron residual concentration of the coagulated effluent decreased with increase in coagulant dose, reaching the lowest levels at OCDs, and then soared with further coagulant addition (Fig. 3(b)). The only exception occurred at pH 6 where iron residual concentration at 1.0 g/L was higher than at 0.75 g/L. In the pH range of 7–9, residual ferric concentration at the OCDs was less than 2% of Fe(III) added, which means that almost all the metal ion introduced is in solid phase (i.e., settling flocs). In comparison, the OCD at pH 6 gave rise to iron residual concentration of about 7% of Fe(III) added. Generally, residual ferric concentration correlates well with residual turbidity, implying the contribution of non-precipitated Fe(III) species to residual turbidity.

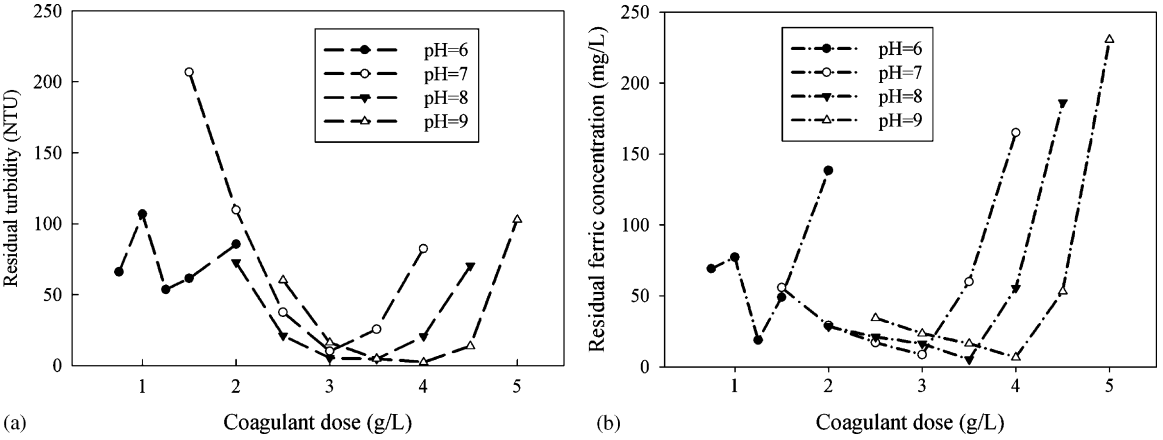

Fig. 3. Residual turbidity and ferric concentration as functions of coagulant dose and pH: (a) turbidity and (b) ferric concentration.

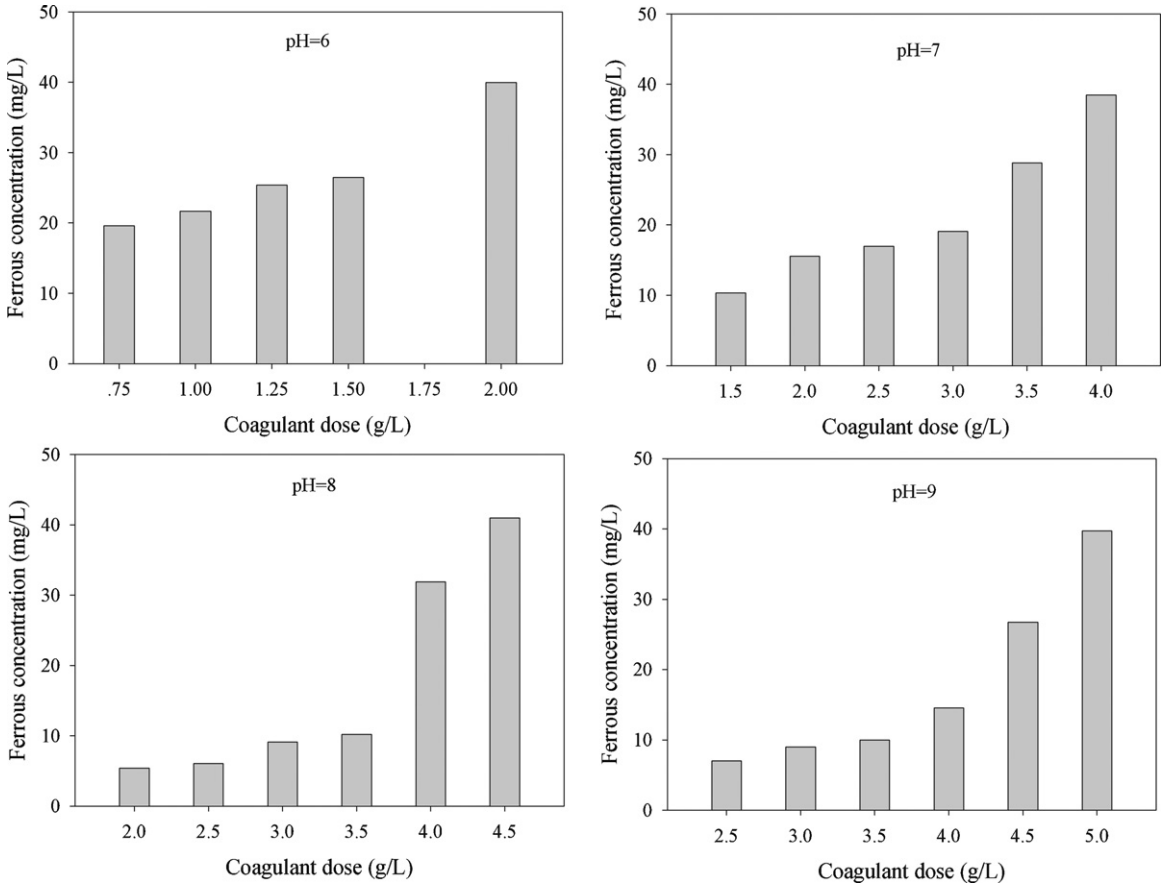

Fig. 4. Ferrous concentration as a function of coagulant dose and pH.

In most cases, residual turbidity at lower coagulant dose was much higher than that of uncoagulated effluent. This negative effect is probably due to the fact that ferric dosage is capable of converting dissolved melanoidins fraction into insoluble form through surface complexation, but not enough for melanoidins–Fe(III) complexes to aggregate into settleable flocs, resulting in elevated residual turbidity and ferric content.

3.4. Effect of coagulant dose and pH on redox potential of Fe(III)

For iron, redox reaction is likely to be involved in addition to hydrolysis process. Fe precipitates to a very large extent in the form of Fe(III). On the other hand, when Fe(III) in solution is reduced into Fe(II) by dissolved organic matters, the tendency for Fe(III) precipitation decreases considerably [18]. NOM-facilitated solubilization of iron in natural water is generally considered to be the result of Fe(III) reduction to Fe(II). Accordingly, ferrous concentration in supernatant was examined as an indirect evidence of potential redox reaction during coagulation process.

Different from ferric residual, residual ferrous concentration shows a tendency of gradual increase with coagulant dose (Fig. 4). Theoretically, the redox potential of Fe^{3+}/Fe^{2+} is +0.771 V under acidic condition, but is negative in alkaline region. Increase in coagulant dosage lowers solution pH towards more acidic region, thus favoring organic removal through redox process, which should account for increasing ferrous content in the finished effluent. Fer-

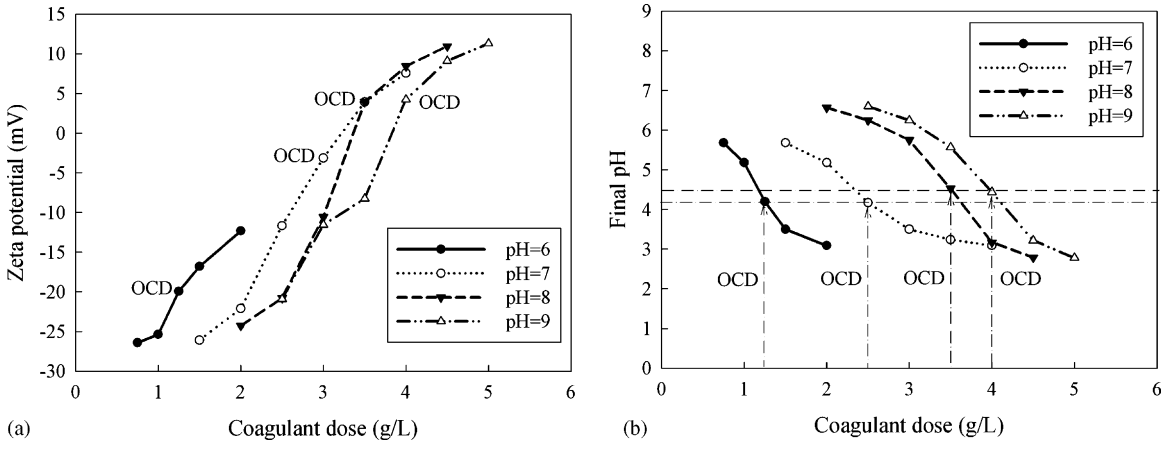

Fig. 5. Zeta potential and final pH as functions of coagulant dose and pH: (a) zeta potential and (b) final pH.

rous concentration at the OCDs accounts for approximately 2% of coagulant added when the value of pH is above 7. This confirms the anti-oxidative property of melanoidins which renders them recalcitrant to not only biological but chemical oxidation.

3.5. Zeta potential and final pH

Melanoidins carry negative charge which is neutralized by cationic Fe(III) hydrolytic species, resulting in rising zeta potential, as shown in Fig. 5(a). There is also marked difference between pH 6 and other pH values. Zeta potentials at the OCDs were in the range of −3 to +4 mV in the pH range of 7–9, indicating minimal net surface charge as a result of charge neutralization. Zeta potentials at pH 6, however, remained negative in the whole dosage range. Even at the OCD, the coagulated effluent was highly negatively charged since zeta potential was only −20 mV.

The curves of final pH (Fig. 5(b)) basically consist of three domains. At pH 8, for instance, pH dropped from 6.6 to 5.8 with increase of coagulant dosage from 2.0 g/L to 3.0 g/L, falling more than 2.5 units in the dosage range of 3.0–4.0 g/L but less than 0.4 unit in the maximal range of 4.0–4.5 g/L. Although hydrolysis of metal salts results in pH relaxation, alkalinity in the effluent functions as an effective pH buffer at lower coagulant dosage. With increasing coagulant dose, especially towards the OCD, rapid consumption of alkalinity by released hydrogen ion leads to sharp decrease in solution pH.

It is noteworthy that despite significant difference in coagulation behavior between initial pH 6 and other pH values, final pH levels at OCDs were squeezed in a narrow range of 4.2–4.6. This suggests that final pH is the most influential factor in the coagulation of bio-treated molasses wastewater using ferric chloride.

3.6. HPSEC chromatograms

Fig. 6(a) presents three different peaks in the raw effluent. Even when ferric salt was underdosed, intensity of the peak I was significantly reduced and the peak II disappeared (Fig. 6(b)). Though the exact molecular weight was not obtained, it is reasonable to postulate that the peak I and II correspond to the high and low molecular weight (MW) fractions of melanoidins, respectively, given that melanoidins is the major organics removed by coagulation. With NOM, it is generally accepted that high MW fractions are more easily removed than low MW fractions [19]. The chromatographic results show that low MW fraction of melanoidins seems to preferentially react with hydrolytic iron species and is destabilized through the formation of insoluble melanoidins–Fe(III) complexes. Though these complexes may not exhibit good settleability, they can be removed by filtration pretreatment of HPSEC. At the same time, the intensity of peak III increased sharply, indicating that the lowest MW fraction is obviously not amenable to removal by coagulation. Manka and Rebhum [20] attributed rising concentration of the lowest MW fraction to the formation of unidentifiable group. Concentration of the high MW fraction continued to diminish with iron dosage while the intensity of peak III soared to more than 35,000 nRIU at the OCD (Fig. 6(c)) and 40,000 nRIU at the maximum dose (4.5 g/L) (Fig. 6(d)). Since increase in coagulant dosage enhances the capacity of charge neutralization (CN), the CN effect is hypothesized to be responsible for rising concentration of the unidentifiable group. The overall process of HPSEC leads to the elution of organic matter in the order of decreasing molecular size. Noticing that elution time of the peak I shortened from 5.7 min (without coagulant) to about 5.1 min (4.5 g/L), it is likely that change in structure or depolymerization associated with destabilization of melanoidins is probably responsible for rising concentration of the unidentifiable group.

3.7. Floc size distribution

Ferric chloride produced a quasi-unimodal size distribution with the mode at approximately 32 μm at 2.0 g/L (Fig. 7). At the OCD, however, this unimodal distribution developed into a bimodal size distribution with a fine mode in the range of 1.6–2.2 μm and a coarse mode at approximately 8 μm. The fine mode consisting of small aggregates is likely to be formed by the low MW fraction of melanoidins. At the maximum dose, the fine mode disappeared, leaving a unimodal (at approximately 34 μm) size distribution similar to that at underdosed coagulant dosage. Disappearance of fine mode suggests that low MW fraction of melanoidins is more likely to restabilize due to charge reversal than high MW fraction when ferric salt is overdosed.

Table 2 presents the statistic results of aggregate size at varying iron dosage. When either underdosed or overdosed, mean floc size was almost the same, compared to much smaller floc size at the OCD. Visual inspection during experiment revealed much clarified supernatant accompanied by low settling rate of flocs. This means that for ferric chloride, the settleability of flocs formed depends on aggregate size with larger flocs settling more rapidly.

3.8. Coagulation mechanism at OCDs

Two mechanisms may explain the coagulation and precipitation behavior of hydrolyzing metal salts: at low pH, charge neutralization of negatively charged particulates by cationic hydrolysis metal species may occur; and at higher coagulant dosages and elevated pH, adsorption of micron particles onto amorphous metal hydroxide flocs followed by precipitation is assumed to play the predominant role [21]. Experimental evidence for such a destabilization mechanism is usually obtained from electrophoretic or zeta potential studies.

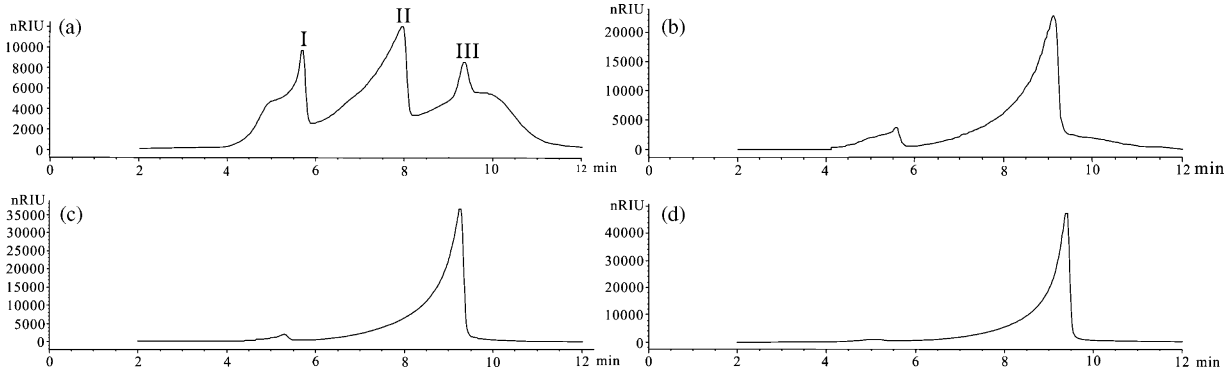

Fig. 6. HPSEC chromatogram of molasses effluent before and after coagulation: (a) raw wastewater, (b) coagulant 2.0 g/L, (c) coagulant 3.5 g/L, and (d) coagulant 4.5 g/L.

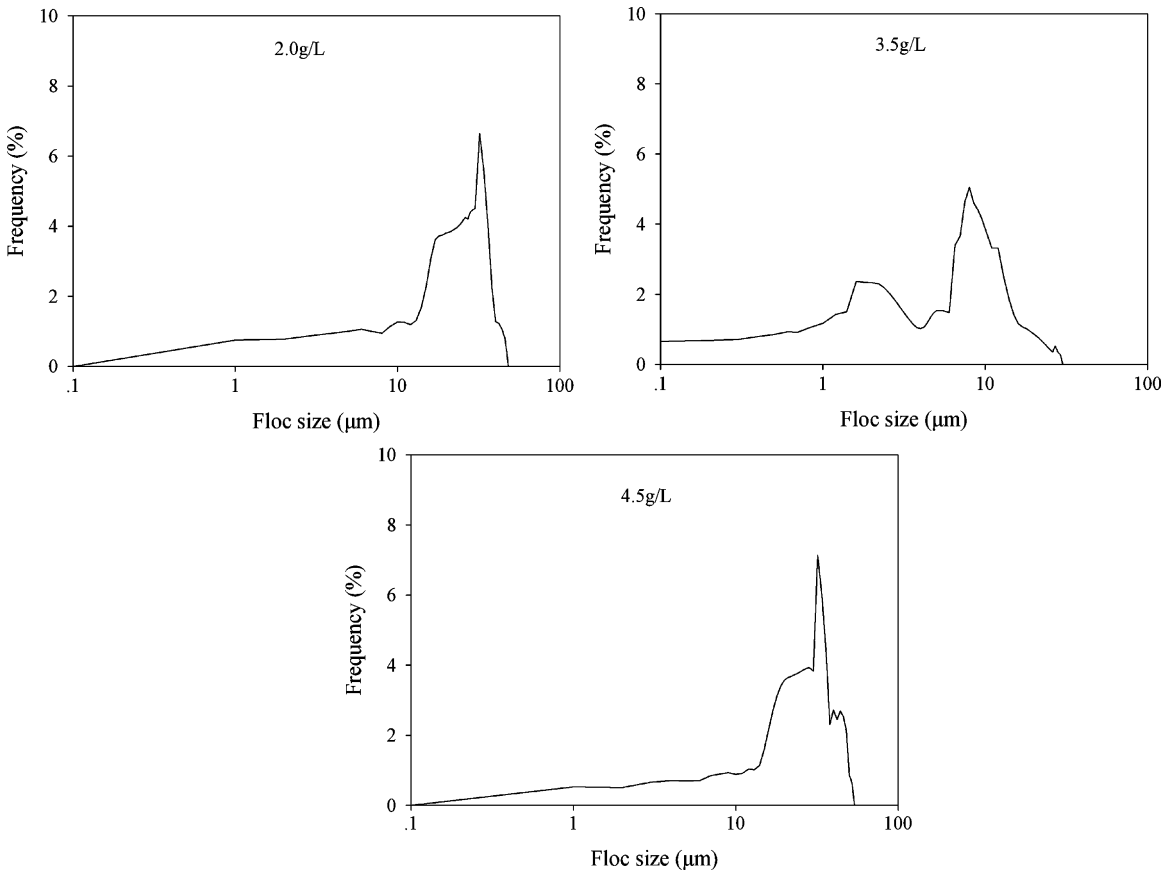

Fig. 7. Floc size distribution of coagulated effluent.

The sign of zeta potential at OCDs in the pH range of 7–9 does suggest charge neutralization mechanism, while charge neutralization is not responsible for the destabilization of melanoidins at pH 6, given still highly negative zeta potential at the OCD. On the other hand, coagulation performance also depends on the extent to which melanoidins can be settled. Since the major portion of melanoidins should be in dissolved form (<0.45 μm), as indicated by relatively low turbidity of the raw effluent, the destabilized particle formed, especially in the case of low MW fraction of melanoidins, may not be able to aggregate into flocs with good settleability. In this regard, the results obtained at pH 6 may shed more light on the coagulation mechanism. The increase of iron dose, especially at the maximum dosage, favors charge neutralization mechanism at pH 6. Therefore, decreasing coagulation performance above the OCD is apparently not due to charge reversal-related restabilization in excess of metal cations, but due to poor settleability of aggregates formed when final pH drops out of the effective range. Since final pH controls the speciation of hydrolysis products of metal salts, this implies that at OCDs, certain amount of high MW hydrolytic Fe(III) species, i.e., ferric hydroxide, is required to serves as nucleating site for soluble Fe–melanoidins complexes to precipitate or to function as bridging agent for primary particles to agglomerate into settleable flocs. The zero point of charge of amorphous ferric hydroxide is about pH 8 [22]. At pH_{OCDs}, the initially formed colloidal precipitate is positively charged and, hence, colloidally stable [23]. This suggests that co-precipitation also plays a vital role in the coagulation of melanoidins from molasses effluent.

Accordingly, the combined effects of charge neutralization and co-precipitation may be responsible for the coagulation of melanoidins from molasses effluent at the OCDs in the pH range of 7–9, while co-precipitation alone plays the predominant role for the destabilization of melanoidins at pH 6. Lack of the ability to effectively neutralize the negative surface charge of melanoidins accounts for worse coagulation performance at pH 6 as compared to that at other pHs.

Table 2
Floc size at varying dosage of ferric chloride.

Coagulant dose (g/L)	2.0	3.5	4.5
Average size (μm)	24.2	6.2	25.8
D_{50} (μm)	27.9	8.4	27.8

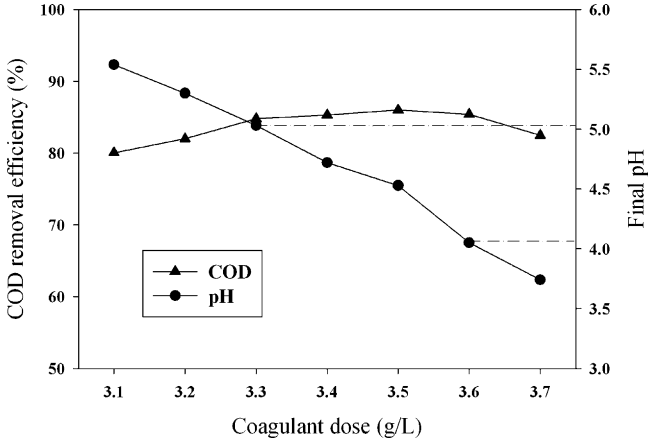

Fig. 8. Optimized COD removal and final pH as functions of coagulant dose.

3.9. Determination of effective pH range

It is necessary to determine the effective final pH range since pH is the most important parameter in the coagulation performance of ferric chloride. This can be achieved by narrowing iron dosage range considering that final pH is usually the consequence of variable coagulant dosage. The result of raw effluent (initial pH 8) is shown in Fig. 8.

COD removal efficiency was initially increased with incrementing ferric addition, reached a plateau in the dosage range of 3.3–3.6 g/L, and then dropped at the maximum dosage (Fig. 8). Consequently, the corresponding pH of 4.1–5.0 is determined as the effective pH range for ferric chloride. This is in good agreement with the optimum pH of 4–5 reported in a numbers of literatures [24,25] for NOM coagulation using ferric chloride.

4. Conclusions

The following conclusions can be obtained from the present study.

1. When ferric chloride is applied in the post-treatment of molasses wastewater, the initial pH value should be above 7 to guarantee effective coagulation efficiency. Under the optimum conditions, i.e., at pH 8 and dosage of 3.5 g/L, ferric salt was able to remove up to 86% of COD and 96% of color from anaerobically–aerobically treated molasses wastewater with residual turbidity less than 5 NTU in the finished effluent.
2. Final pH is the predominant factor in determining coagulation performance and the effective pH range is around 4–5 for ferric chloride. Measurement of ferrous concentration indicates that removal of melanoidins is mostly via coagulation process. Only when solution pH tends towards acidic, does redox reaction become increasingly important.
3. HPSEC results indicate that the low MW fraction of melanoidins preferentially reacts with Fe(III) species. Increase in concentration of the lowest MW organic group is related to the capacity of charge neutralization.
4. Floc size measurement reveals unimodal floc size distribution for underdosed and overdosed coagulant but bimodal distribution at the optimal dosage. The settling rate of flocs formed is largely determined by aggregates size with larger flocs settling more rapidly.
5. Under the optimum conditions, combined effect of charge neutralization and co-precipitation is the predominant coagulation mechanism when pH is above neutral using ferric chloride, while co-precipitation alone plays the predominant role at pH 6.

Acknowledgements

The research work was financially supported by National Natural Science Foundation of China (Grant No. 40830748), China Postdoctoral Science Foundation (Grant No. 20080440976) and Ministry of Environmental Protection of China.

References

[1] M.L. Wolfrom, D.N. Kolb, A.W. Langer, Chemical interactions of amino compounds and sugars. VII, pH dependency, J. Am. Chem. Soc. 75 (1953) 3471–3473.
[2] M. Peña, G. González, N. San, C. Heras, Color elimination from molasses wastewater by *Aspergillus niger*, Bioresour. Technol. 57 (1996) 229–235.
[3] M. Coca, M. Peña, G. González, Variables affecting efficiency of molasses fermentation wastewater ozonation, Chemosphere 60 (2005) 1408–1415.
[4] S.H. Mutlua, U. Yetisb, T. Gurkana, L. Yilmaza, Decolorization of wastewater of a baker's yeast plant by membrane processes, Water Res. 36 (2002) 609–616.
[5] M. Peña, M. Coca, G. González, R. Rioja, M.T. García, Chemical oxidation of wastewater from molasses fermentation with ozone, Chemosphere 51 (2003) 893–900.
[6] A. Pala, G. Erden, Decolorization of a baker's yeast industry effluent by Fenton oxidation, J. Hazard. Mater. B127 (2005) 141–148.
[7] M. Goto, T. Nada, A. Ogata, A. Kodama, T. Hirrose, Supercritical water oxidation for the destruction of municipal excess sludge and alcohol distillery wastewater of molasses, J. Supercrit. Fluid. 13 (1998) 277–282.
[8] A. Ikuko, T. Yukiko, O. Sadahiro, U. Kiyimoto, Production of decolorizing activity for molasses pigment by *Coriolus versicolor* Ps4a, Biol. Chem. 49 (1985) 2041–2045.
[9] K.F. Fannin, J.R. Conrad, V.J. Srivastava, D.P. Chynoweth, D.E. Jerger, Anaerobic treatment of winery wastewater, J. Water Pollut. Control Fed. 59 (1987) 403–410.
[10] S.C. Jones, F. Sotiropoulos, A. Amirtharajah, Numerical modeling of helical static mixers for water treatment, J. Environ. Eng. ASCE 128 (2002) 431–440.
[11] W. Zhao, Y.P. Ting, J.P. Chen, C.H. Xing, S.Q. Shi, Advanced primary treatment of wastewater using a bio-flocculation–adsorption sedimentation process, Acta Biotechnol. 20 (2000) 53–64.
[12] Y.X. Wang, Z. Liang, X.M. Yuan, Y.S. Xu, Preparation of cellular iron using wastes and its application in dyeing wastewater treatment, J. Porous Mater. 12 (2005) 225–232.
[13] V. Migo, M. Matsumura, E.J. Rosario, H. Kataoka, Decolorization of molasses wastewater using an inorganic floculant, J. Fermentation Bioeng. 75 (1993) 438–442.
[14] D. Ryan, A. Gadd, J. Kavanagh, M. Zhou, G. Barton, A comparison of coagulant dosing options for the remediation of molasses process water, Sep. Purif. Technol. 58 (2008) 347–352.
[15] APHA, Standard Methods for the Examination of Water and Wastewater, 19th edition, American Public Health Organization, Washington, DC, USA, 1995.
[16] A. Amokrane, C. Comel, J. Veron, Landfill leachates pretreatment by coagulation–flocculation, Water Res. 31 (1997) 2775–2782.
[17] E. Lefebvre, B. Legube, Iron (III) coagulation of humic substances extracted from surface waters: effect of pH and humic substances concentration, Water Res. 24 (1990) 591–606.
[18] K.G. Nierop, B. Jansen, J.M. Verstraten, Dissolved organic matter, aluminium and iron interactions: precipitation induced by metal/carbon ratio, pH and competition, Sci. Total Environ. 300 (2002) 201–211.
[19] A. Matilainen, N. Lindqvist, S. Korhonen, T. Tuhkanen, Removal of NOM in the different stages of the water treatment process, Environ. Int. 28 (2002) 457–465.
[20] J. Manka, M. Rebhum, Organic groups and molecular weight distribution in tertiary effluents and renovated waters, Water Res. 16 (1982) 399–403.
[21] R.L. Sinsabaugh, R.C. Hoehn, W.R. Knocke, A.E. Linkins, Removal of dissolved organic carbon by coagulation with iron sulfate, J. Am. Water Works Assoc. 78 (1986) 74–82.
[22] M.I. Aguilar, J. Sáez, M. Lloréns, A. Soler, J.F. Ortuño, V. Meseguer, A. Fuentes, Improvement of coagulation–flocculation process using anionic polyacrylamide as coagulant aid, Chemosphere 58 (2005) 47–56.
[23] J. Duan, J. Gregory, Coagulation by hydrolysing metal salts, Adv. Colloid Interface 100–102 (2003) 475–502.
[24] E.S. Hall, R.F. Packham, Coagulation of organic color with hydrolyzing coagulants, J. Am. Water Works Assoc. 57 (1965) 1149–1163.
[25] A. Amirtharajah, K.E. Dennett, A. Studstill, Ferric chloride coagulation for removal of dissolved organic matter and trihalomethane precursors, Water Sci. Technol. 27 (1993) 113–121.